Available online at www.sciencedirect.com
ScienceDirect
Journal of Power Sources 175 (2008) 250–255
JOURNAL OF POWER SOURCES
www.elsevier.com/locate/jpowsour

Short communication

Pt/C doped by MoO_x as the electrocatalyst for oxygen reduction and methanol oxidation

N.R. Elezović [a], B.M. Babić [b], V.R. Radmilović [c], S. Lj. Gojković [d], N.V. Krstajić [d], Lj.M. Vračar [d,*]

[a] *Center for Multidisciplinary Studies, University of Belgrade, Serbia*
[b] *Vinča Institute of Nuclear Sciences, Belgrade, Serbia*
[c] *National Center for Electron Microscopy, LBLN University of California, Berkely, USA*
[d] *Faculty of Technology and Metallurgy, University of Belgrade, Serbia*

Received 16 July 2007; received in revised form 21 August 2007; accepted 5 September 2007
Available online 14 September 2007

Abstract

The oxidation of methanol and reduction of oxygen were studied on MoO_x–Pt/C nano-catalysts prepared by the polyole method combined by MoO_x post-deposition. The catalysts were characterized by TEM and EDX. The presented composition of the electrode is very similar to the nominal ones and post-deposited MoO_x species block only a small fraction of the active Pt particle surface area. MoO_x deposition on the carbon support can be ruled out from the EDX results and the low mobility of these oxides at corresponding conditions. The electrode catalytic activity in the electrooxidation of methanol and the reduction of oxygen was studied by steady-state voltammetry and cyclic voltammetry. MoO_x–Pt/C catalyst exhibits higher catalytic activity than Pt/C for the oxygen reduction. The catalytic effect in oxidation of methanol is achieved only under potentiodynamic conditions, when poisoning species have no enough time to develop fully.

Keywords: Methanol oxidation; Oxygen reduction; Platinum; Molybdenum oxides; TEM

1. Introduction

Platinum is the most active single metal catalyst for many electrochemical reactions among which are oxygen reduction (ORR) and methanol oxidation (MOR). However, onset potentials of both reactions are rather far from their thermodynamic values. Besides, Pt is readily poisoned by CO, what impairs its performance as an anode both in direct methanol fuel cell (DMFC) and in H_2/O_2 proton exchange fuel cell (PEFC) working with reformate gas. A lot of research effort has been done to solve these problems by the addition of a second metal to Pt.

Nano-sized Pt–Ru catalyst was found to be the most effective as the anode catalyst in direct methanol fuel cell (DMFC) [1]. Other metals and their oxides have also been tested, but there is no general agreement so far that any of them excel Ru. Bulk Pt–Mo [2] and nano-sized Pt–Mo alloys [3] were found to posses high CO-tolerance in oxidation of H_2/CO mixtures. The similar results were reported for MoO_x–Pt/C with MoO_x as an amorphous oxide phase [4]. However, the results on the effect on MOR are not straightforward. It was reported [5] that performance of a DMFC fuel cell anode with Pt and PtRu black as the catalysts was even worse after the modification with Mo oxide. Preliminary results by Urian et al. [6] show that Pt–Mo alloys with the atomic composition of 3:1 and 4:1 (Pt:Mo ratio) do not exhibit any enhancement of MOR in contrast to their excellent CO tolerance abilities. On the other hand, enhanced activity for MOR has been recently reported [7] on Pt/MoO_x/C composite electrodes prepared by an electrochemical co-deposition technique using a glassy carbon electrode as a substrate. In this study the enhancement of the methanol oxidation rate was ascribed to the existence of the Mo(VI)/Mo(IV) redox couple in the substoichiometric lower valence MoO_x ($2 < x < 3$) and a possibility of a proton spillover effect from hydrogen molybdenum bronze. Therefore, the effects of the precursors, preparation method, and heat treatment on the catalytic activity of MoO_x–Pt/C for MOR remain to be explored.

* Corresponding author. Tel.: +381 11 3303 685; fax: +381 11 3370 387.
E-mail address: ljvracar@tmf.bg.ac.yu (Lj.M. Vračar).

0378-7753/$ – see front matter © 2007 Elsevier B.V. All rights reserved.
doi:10.1016/j.jpowsour.2007.09.011

Alloys of Pt with other metals, mostly first raw transition metals as Co, Ni, Cr, V and Fe, were found to be more active for ORR than pure Pt [8–15] and they have to be sintered above 700 °C to achieve chemical stability. The effect of transition metal was explained through the inhibition of the OH adsorption on Pt surface by the alloying metal [11], the geometric modification of Pt [8], extensive surface roughening [10], as well as through the lowering the strength of adsorbed oxygen species because of the electronic interactions [8,9]. Enhanced activity for ORR was also reported for composites like Pt–MO_x (M = Ti and W) [16–18].

However, no investigation of ORR on MoO_x–Pt/C electrodes was reported so far. By mixing MoO_x with Pt nanoparticles we expected the change in the oxygen reduction rate through the modification of the 5-d orbital vacancies of Pt atoms, or through the reduction of Pt reactivity for OH adsorption due to the presence of Mo that could have one or more OH ligands attached on it.

2. Experimental

2.1. Catalyst preparation

Pt/C catalysts were prepared by modified ethylene glycol (EG) method on high area carbon (Vulcan XC-72). The details of preparation procedure were reported elsewhere [19]. In brief, hexachloroplatinic (IV) acid (H_2PtCl_6) solution was dissolved in water solution of EG and pH was adjusted to 12 by NaOH. This solution was added dropwise under mechanically stirred condition to the suspension of carbon in EG solution and the mixture was heated to 160 °C for 2 h to allow platinum salt being reduced to platinum metal. The whole preparation process was conducted in argon atmosphere. After filtration and washing, the filter cake was dried in a vacuum at 60 °C for 12 h. The Pt loading of the catalysts were always 16.6 wt.%. The Pt/C catalysts were finally heat treated at 300 °C under H_2 atmosphere for 1 h. In order to dope Pt/C with MoO_3, the Pt/C powder was suspended in water and appropriate amount of sodium molybdate was dissolved to obtain the Pt:MoO_3 molar ratio of 80:20. Then, excess conc. HCl was added into this suspension. Nanoscale molybdenum oxide particles were produced by the reaction of sodium molybdate with HCl. The solution was stirred for 24 h at the ambient temperature to adsorb molybdenum oxide on the Pt/C. The MoO_3–Pt/C catalysts were finally heat treated at 300 °C under H_2 atmosphere for 1 h.

2.2. Electrochemical cell and electrode preparation

A conventional three-compartment all glass cell was used. The working electrode compartment was separated from other two by fritted glass discs. The counter electrode was a platinum sheet of 5 cm^2 geometric area. The reference electrode was a Pt/H_2 electrode in the same solution (ORR experiments) or saturated calomel electrode (MOR experiments). All potentials were referred to the reversible hydrogen electrode (RHE). ORR was investigated in 0.5 mol dm^{-3} $HClO_4$ solution while the methanol oxidation reaction was investigated in 0.1 mol dm^{-3} H_2SO_4 + 0.1 mol dm^{-3} methanol solution.

Two milligrams of MoO_x–Pt/C catalyst was ultrasonically suspended in 1.0 ml of water and 50 μl of Nafion solution (5 wt.%, Aldrich) to prepare catalyst ink. Then, 15.0 μl of ink was transferred with an injector to a gold disk (6 mm diameter) of the rotating disk electrode assembly, so the Pt loading of the catalyst was 5 μg. After the water volatilization, the electrode was heated at 80 °C for 10 min.

2.3. Electrode characterization

Transmission electron microscopy (TEM) measurements were performed using the FEI (Fillips electronic instruments)-CM200 super-twin and CM300 ultra-twin microscopes operating at 200 and 300 kV and equipped with the Gatan 1k × 1k and 2k × 2k CCD cameras, respectively. Particle size distributions were determined from images of, on average, 20 different regions of the catalyst; each region contained 10–20 particles. The particle shapes were determined by real space crystallography with the use of high-resolution images taken from particles near or on the edge of the carbon black substrate, and/or by numerical Fourier filtering of the digitized image intensity spectrum of particles on top of the carbon.

Electrochemical characterization was performed on an EG&G273 instrument. Cyclic voltammetry was performed in 0.5 mol dm^{-3} $HClO_4$ saturated with high purity nitrogen that was continuously bubbling through the working electrode compartment.

3. Results and discussion

3.1. TEM analysis

Representative TEM images of the MoO_x–Pt/C catalyst as well as the corresponding particle size distribution are presented in Fig. 1. As evident from Fig. 1, the Pt–MoO_x nanoparticles are homogenously distributed over the carbon support, with no evidence for pronounced particle agglomeration. The quite similar particle size and size distribution was obtained for Pt/C catalyst. Both catalyst samples show monomodal particle size distribution with the mean particle sizes of 2.5 nm. These results confirm that MoO_x post-deposition does not lead to a growth of the Pt nanoparticles.

The distribution of MoO_x deposit on the Pt nanoparticles cannot be derived from the TEM images. The elemental compositions of the corresponding catalysts (in mol%) derived from the EDX measurements are listed in Table 1. C represents the majority component, in agreement with the nominal Pt content of about 16.6 wt.% and the molar masses of Pt, MoO_x and C. Three to 4 at.% of oxygen are attributed to Mo oxides, as well as to surface oxidation of carbon support during conditioning of the catalysts and during subsequent storing before the sample analysis. Correspondingly, no metallic molybdenum signal is detected on Pt–MoO_x catalyst by the X-ray analysis, supporting the above conclusion that the MoO_x surface modification process

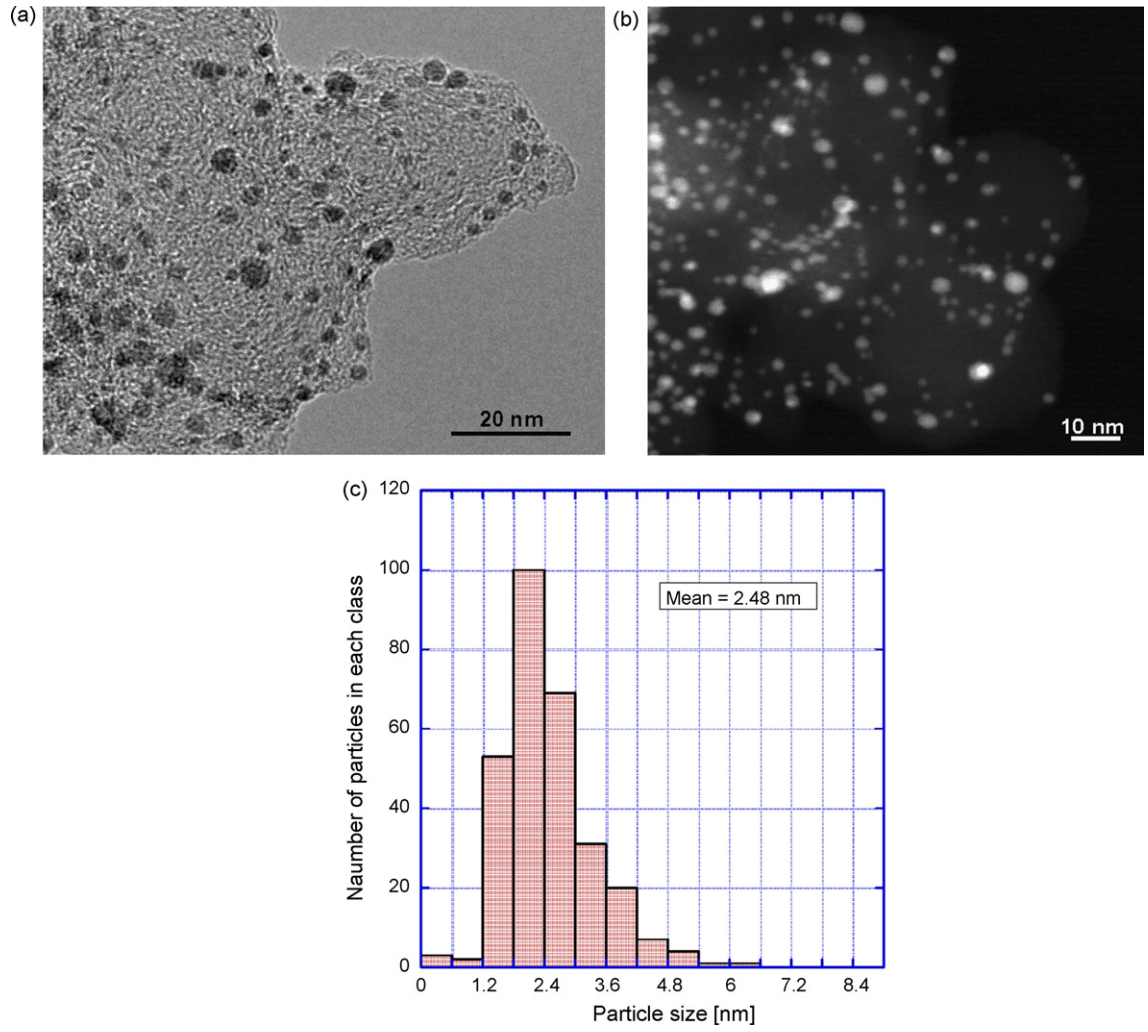

Fig. 1. (a) HRTEM micrographs of MoO_x–Pt nanoparticles on carbon support. (b) High angle annular dark field (HAADF) image. (c) The corresponding histogram of particle size distribution.

and subsequent treatment do not lead to bulk alloy formation. The treatment of the samples during preparation procedure at 300 °C in hydrogen atmosphere and at cathodic reaction potentials do not exclude partial molybdenum oxides reduction, while alloy formation under reaction conditions appears unlikely due to low temperature.

3.2. Cyclic voltammetry

To gain further insight on the distribution of the MoO_x species on the Pt nanoparticle surface, we determined the active surface area of the catalysts under study by cyclic voltammetry. The experiments were done in 0.5 mol dm^{-3} $HClO_4$ saturated with high purity nitrogen that was continuously bubbling through the working electrode compartment. The potential was cycled from 0.03 to 1.30 V (RHE) at the sweep rate of 100 mV s^{-1}. The results for MoO_x–Pt/C are presented and compared with Pt/C in Fig. 2. The double layer region is well defined with a clear separation among hydrogen, oxygen and double layer regions, which is typical behavior of Pt in acid solution. A stable response was found after few cycles with no current of Mo oxidation or dissolution for potentials up to 1.30 V. This indicates that the MoO_x particles are stabilized by the interactions with neighboring Pt atoms. The redox pair observed at ca. 0.45 V could be attributed to the intermediate oxidation states of Mo, being between III and IV.

Table 1
Particle size and chemical composition of MoO_x–Pt/C catalyst

Weight (%)	C(K): 76.6; O(K): 3.09; Mo(K): 1.91; Pt(L): 18.4
Atomic (%)	C(K): 95.4; O(K): 2.89; Mo(K): 0.298; Pt(L): 1.41
Nominal content (Mo/Pt at.%)	16.6
Determined by EDX (Mo/Pt at.%)	21.1
Particle size (nm)	2.5

The active surface areas determined from hydrogen-UPD adsorption/desorption region for the MoO_x–Pt/C and Pt/C catalysts, listed in Table 2 show that after the modification of the catalyst by MoO_x, only about 23% of the Pt active surface area was blocked. Assuming that Pt particles are spherical, their dispersion is about 21%. If modification by 20 mol% MoO_x

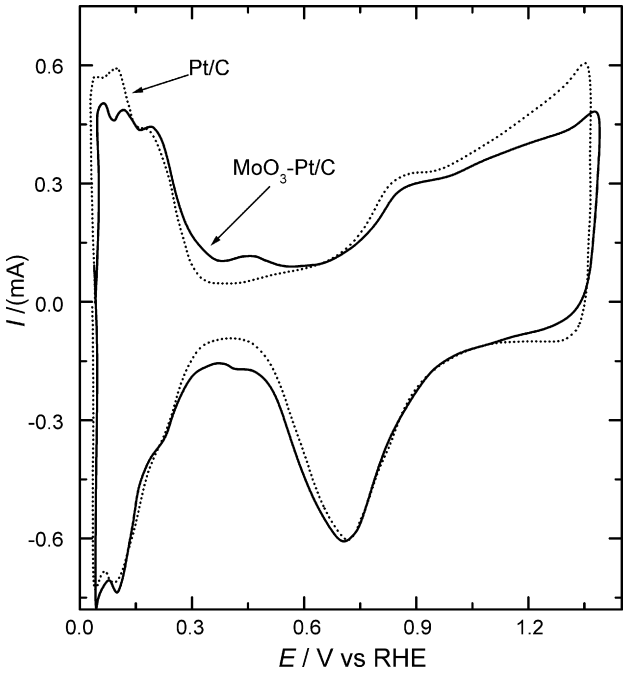

Fig. 2. Cyclic voltammograms of Pt/C and MoO_x–Pt/C catalysts in 0.5 mol dm^{-3} $HClO_4$ solution at 293 K, with sweep rate of 100 mV s^{-1}.

produced a monolayer of Mo, the surface area of Pt particles would be decreased for about 95% and even more in the case of the monolayer of MoO_x. Since the actual loss in active surface area is significantly smaller than that, it can be concluded that MoO_x particles are agglomerated on the Pt nanoparticle surface in small three-dimensional islands with a height of several monolayers. EDX analysis conducted at 15 different places of the catalyst showed that the presence of the MoO_x was always followed by the presence of Pt species whose molar ratio did not vary significantly from the nominal one. So, MoO_x deposition on the carbon support could be ruled out from the EDX results.

3.3. Methanol oxidation reaction (MOR)

First potential sweeps in methanol containing solution recorded on Pt/C and MoO_x–Pt/C electrocatalysts at 50 mV s^{-1} are presented in Fig. 3. As one can see, methanol oxidation commences at about 0.4 V, irrespectively on the presence of MoO_x. At the potentials more positive than 0.5 V the current densities on MoO_x–Pt/C become higher and reach the maximum value earlier than on Pt/C electrode. In the subsequent sweeps (not shown), the methanol oxidation rate slowly decreased and after about 10 cycles a steady state was achieved. Over that time the maximum current densities dropped from 0.82 to 0.72 mA cm^{-2} and from

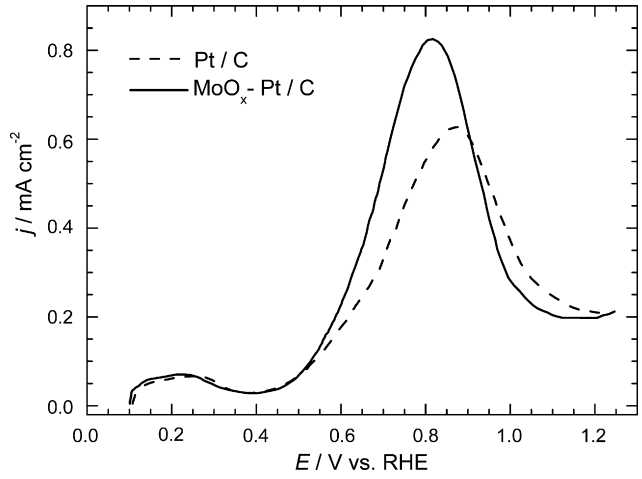

Fig. 3. First potential sweeps of Pt/C and MoO_x–Pt/C electrodes in 0.1 mol dm^{-3} CH_3OH + 0.1 mol dm^{-3} H_2SO_4 solution at 50 mV s^{-1}.

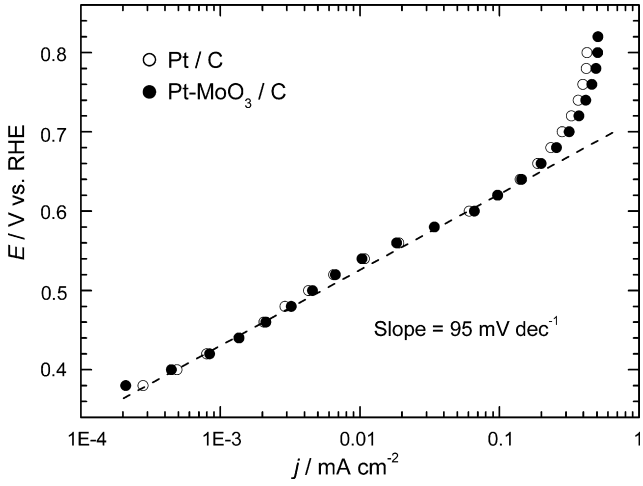

Fig. 4. Polarization curves for methanol oxidation at Pt/C and MoO_x–Pt/C electrodes in 0.1 mol dm^{-3} CH_3OH + 0.1 mol dm^{-3} H_2SO_4 solutions.

0.62 to 0.48 mA cm^{-2} on MoO_x–Pt/C and Pt/C, respectively. However, polarization curves for MOR on Pt/C and MoO_x–Pt/C recorded at 1 mV s^{-1} completely overlap (Fig. 4).

Methanol oxidation follows a complex mechanism which includes strongly adsorbed CO_{ads}, CHO_{ads}/COH_{ads} and soluble HCHO and HCOOH [20]. Between 0.2 and 0.5 V Mo is in intermediate oxidation states (III and IV) and is capable to promote oxidation of weakly bound CO_{ads} [21]. Consequently, in this potential region modification of Pt with MoO_x did not show any influence to MOR. However, at the potentials more positive than 0.5 V the enhancement of the MOR current densities was observed (Fig. 3). According to the anodic peak on

Table 2
Kinetic parameters for the oxygen reduction reaction obtained in 0.5 M $HClO_4$ at 25 °C for Pt/C and MoO_x–Pt/C catalysts

Catalyst	Electrochemically active surface area (m^2 g^{-1} Pt)	Tafel slope (mV dec^{-1})		Mass activity at 0.85 V vs. RHE (mA mg^{-1} Pt)	Specific activity at 0.85 V vs. RHE (mA cm^{-2} Pt)
Pt/C	96	−67	−132	32	0.035
MoO_x–Pt/C	74	−65	−128	89	0.120

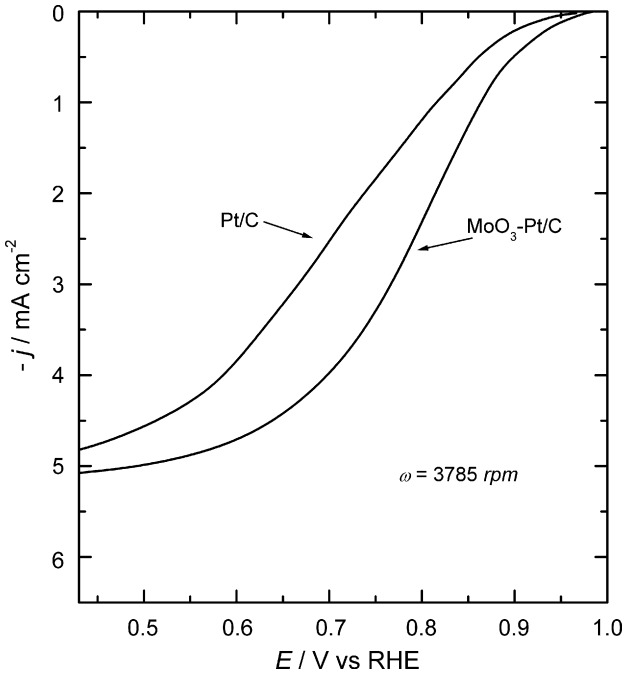

Fig. 5. Polarization curves obtained with rotating disk electrode for O_2 reduction in 0.5 mol dm^{-3} $HClO_4$ solution at Pt/C and Mo_x–Pt/C electrodes at 3785 rpm.

the cyclic voltammogram of the MoO_x–Pt/C electrode (Fig. 2), in that potential region Mo is completely oxidized to Mo(VI) species, which was found to be inactive for oxidation of strongly bound CO_{ads} [21]. The negative shift of the maximum potential indicates that formation of Pt-oxide is facilitated in the presence of Mo(VI) what could be caused by a certain spillover of oxygen from MoO_x or its hydrous form to Pt atoms. It seems that this effect can help in oxidation of methanol residues other than strongly bound CO_{ads}, but only under the potentiodynamic conditions, when poisoning species have no enough time to develop fully.

3.4. Oxygen reduction reaction

The activity of MoO_x–Pt/C catalyst towards ORR was tested by the rotating disk electrode measurements and compared to the activity of the Pt/C catalyst. Polarization curves recorded from the open circuit potential by the linear sweep at the rate of 20 mV s^{-1} in 0.5 mol dm^{-3} $HClO_4$ solution, are given in Fig. 5. The onset potential is more positive on MoO_x–Pt/C electrode and ORR is faster in the entire potential range than on Pt/C electrode. The half-wave potential is 90 mV more positive on MoO_x–Pt/C than on Pt/C catalyst. A small difference between the limiting current densities on the two electrodes is probably due to the difference in geometric surface area of the catalyst layer on the supporting gold disk. Thus, it can be assumed that the number of electrons exchanged per O_2 molecule is the same on both catalysts.

The kinetic currents for ORR calculated from the intercepts of the $1/I - 1/\omega^{1/2}$ lines (Koutecky–Levich plot) and normalized to the previously determined electrochemically active surface area of Pt particles, are presented as the Tafel plot in Fig. 6. Both electrodes are characterized with two Tafel slopes, whose

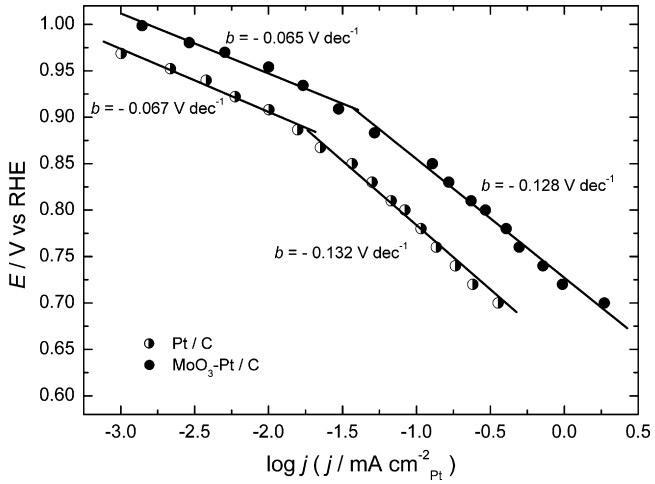

Fig. 6. Tafel plots normalized to the electrochemically active surface area for O_2 reduction in 0.5 mol dm^{-3} $HClO_4$ solutions at Pt/C and MoO_x–Pt/C electrodes.

values are presented in Table 2. At low current densities slopes are close to $-2.3\ RT/F$ and at high current densities close to $-2.3 \times 2RT/F$, as usually referred for both polycrystalline [22] and nano-sized Pt [23] in aqueous solution. This indicates that the reaction mechanism is likely to be the same on MoO_x–Pt/C and Pt/C catalysts, i.e. the first charge transfer as rate determining in both current densities regions but under Temkin adsorption conditions in the low and Langmuirian conditions in the high current densities region [22].

It is common to compare the value of the kinetically controlled current densities at a potential of 0.85 V (RHE), where influences of mass transport are negligible. In our experiments the values of the specific current densities at constant potential for these two electrodes are quite different with significant enhancement in oxygen reduction activity for MoO_x–Pt/C (Table 2). The similar specific current densities for ORR at Pt/C electrode were already reported in the literature [23–27]. Gasteiger et al. in their review paper [28] listed the activities for different Pt/C catalysts, whose surface areas were >60 m^2 g^{-1} Pt, too. The values of $j_{(0.9\,V)} > 200$ μA cm^{-2} Pt are reported for the temperature between 65 and 80 °C. Taking into account, literature reported value for the apparent enthalpy of activation, for ORR, in the low current density region of 60 kJ mol^{-1}, or in the high current density region of 41 kJ mol^{-1} [29–31], on one hand, and current dependence on potential, on the other hand, we calculated that specific activity for our Pt/C catalyst at 0.90 V for the temperature of 80 °C should be 274 or 256 μA cm^{-2} Pt, respectively, which is in a good agreement with listed results.

The increase of the catalytic activity of MoO_x–Pt/C catalyst could be explained through the increase of the number of active sites for the ORR or by synergetic effects due to the formation of the interface between the platinum and oxide materials and by spillover due to surface diffusion of intermediates.

The results presented above show promising increase in specific catalytic activity for oxygen reduction, and illustrate that mixing MoO_3 with Pt nanoparticles changes the oxygen reduction rate, as we expected.

4. Conclusions

MoO_x–Pt/C nano-catalyst was prepared by post-deposition of MoO_x at room temperature from sodium molybdate. Cyclic voltammetry investigations show that post-deposited MoO_x species block only a small fraction of the electrochemically active Pt particle surface area.

The negative shift of the maximum potential for methanol oxidation indicates that formation of Pt-oxide that is facilitate in the presence of MoO_x could be caused by a certain spillover of oxygen from MoO_x to Pt atoms. It seems that this effect can help in oxidation of methanol residues other than strongly bound CO_{ads}, but only under the potentiodynamic conditions, when poisoning species have no enough time to develop fully.

MoO_x–Pt/C nano-catalyst exhibits higher catalytic activity for the oxygen reduction reaction than Pt/C, which is attributed to the synergetic effects due to formation of an interface between the platinum and MoO_x, and by spillover due to diffusion of the reaction intermediates.

Acknowledgement

This paper has been supported by the Ministry of Science, Republic of Serbia, under contract no. 142038.

References

[1] S. Wasmus, A. Küver, J. Electroanal. Chem. 461 (1999) 14.
[2] B.N. Grgur, G. Zhuang, N.M. Markovic, P.N. Ross, J. Phys. Chem. B 101 (1997) 3910.
[3] B.N. Grgur, N.M. Markovic, P.N. Ross, J. Electrochem. Soc. 146 (1999) 1613.
[4] T. Ioroi, N. Fujiwara, Z. Siroma, K. Yasuda, Y. Miyazaki, Electrochem. Commun. 4 (2002) 442.
[5] C. Song, M. Khanfar, P. Pickup, J. Appl. Electrochem. 36 (2006) 339.
[6] R.C. Urian, S. Mukerjee, C. Witham, S. Narayanan, T. Valdez, Extended Abstracts of the Electrochemical Society Spring Meeting, Symposium on Direct Methanol Fuel Cells, March 25–30, 2001.
[7] Y. Zhang, E.R. Wang, Fachini, C.R. Cabrera, Electrochem. Solid State Lett. 2 (1999) 437.
[8] S. Mukerjee, S. Srinivasan, M.P. Soriaga, J. Electrochem. Soc. 142 (1995) 1409.
[9] T. Toda, H. Igarashi, H. Uchida, M. Watanabe, J. Electrochem. Soc. 146 (1999) 3750.
[10] M.T. Paffett, J.G. Beery, S. Gottesfeld, J. Electrochem. Soc. 135 (1988) 1431.
[11] U.A. Paulus, A. Wokaun, G.G. Sherer, T.J. Shmidt, V. Stamenkovic, V. Radmilovic, N.M. Markovic, P.N. Ross, J. Phys. Chem. B 106 (2002) 4181.
[12] U.A. Paulus, A. Wokaun, G.G. Scherer, T.J. Schmidt, V. Stamenkovic, N.M. Markovic, P.N. Ross, Electochim. Acta 47 (2002) 3787.
[13] F.H.B. Lima, M.J. Giz, E.A. Ticianelli, J. Braz. Chem. Soc. 16 (2005) 328.
[14] L. Xiong, A.M. Kannan, A. Manthiram, Electrochem. Commun. 4 (2002) 898.
[15] F.H.B. Lima, W.H. Lizcano-Valbuena, E. Teixeira-Neto, F.C. Nart, E.R. Gonzalez, E.A. Ticianelli, Electrochim. Acta 52 (2006) 385.
[16] H.C. Chiu, A.C.C. Tseung, Electrochem. Solid State Lett. 2 (1999) 379.
[17] O. Savadogo, P. Beck, J. Electrochem. Soc. 143 (1996) 3842.
[18] J. Shim, C. Lee, H. Lee, J. Lee, E.J. Cairns, J. Power Sources 102 (2001) 172.
[19] B.M. Babić, Lj.M. Vračar, V. Radmilović, N.V. Krstajić, Electrochim. Acta 51 (2006) 3820.
[20] T.D. Jarvi, E.M. Stuve, in: J. Lipkowski, P.N. Ross (Eds.), Electrocatalysis, Wiley–VCH, New York, 1998.
[21] G. Samjeské, H. Wang, T. Löffler, H. Baltruschat, Electrochim. Acta 47 (2002) 3681.
[22] D.B. Sepa, M.V. Vojnovic, A. Damjanovic, Electrochim. Acta 26 (1981) 781.
[23] U.A. Paulus, T.J. Schmidt, H.A. Gasteiger, R.J. Behm, J. Electroanal. Chem. 495 (2001) 134.
[24] M. Watanabe, K. Makita, U. Hiroyuki, S. Motoo, J. Electronal. Chem. 197 (1986) 195.
[25] J. Bett, J. Lundquist, Electrochim. Acta 18 (1973) 343.
[26] S. Mukerjee, S. Srinivasan, J. Electroanal. Chem. 357 (1993) 201.
[27] F. Gloaguen, P. Convert, S. Gamburzev, O.A. Velev, S. Srinivasan, Electrochim. Acta 43 (1998) 3767.
[28] H.A. Gasteiger, S.S. Kocha, B.S. Sompalli, F.T. Wagner, Appl. Catal. B: Environ. 56 (2005) 9.
[29] D.B. Sepa, M.V. Vojnovic, Lj.M. Vracar, A. Damjanovic, Electrochim. Acta 31 (1986) 91.
[30] N. Wakabayachi, M. Takeichi, H. Uchida, M. Watanabe, J. Phys. Chem. B 109 (2005) 5836.
[31] N. Wakabayachi, M. Takeichi, M. Itagaki, H. Uchida, M. Watanabe, J. Electroanal. Chem. 574 (2005) 339.